SYSTEM HYDROLOGY TOOLS FOR THE UPPER CATCHMENTS OF THE JORDAN RIVER AND LAKE KINNERET, ISRAEL

Alon Rimmer, Israel Oceanographic & Limnological Research Ltd.

The Yigal Allon Kinneret Limnological Laboratory,

P.O. Box 447 Migdal 14950 Israel,

e-mail: alon@ocean.org.il

Submitted to the Fifth biennial Rosenberg International Forum on Water Policy

September 6-11, 2006, Banff, Canada.

May 2006

ABSTRACT

Three studies on major hydrological problems in the Upper Catchments of the Jordan River and Lake Kinneret, Israel, are reported. By application of system approach to each problem we learned the nature of each system and the major physical laws that govern its operation. The studies were focused on: 1. **Identify** the hydrological system (precipitation – stream flow relations) of the Jordan River sources, that originate from the karstic region of Mt. Hermon; 2. **Detection** of three unknown components: evaporation, saline springs discharge and salinity, of the monthly water-solute-heat balances of Lake Kinneret, and 3. Long-term **predictions** of Lake Kinneret salinity, in response to operational changes such as reduced inflows. Each system is presented from the description of the problem, through the mathematical justifications and equations, to the results and discussion.

1. INTRODUCTION

System approach in hydrology

The approaches to the study of hydrological problems can be generally divided into two extreme groups (Amorocho and Hart, 1964): (1) physical science approach and (2) systems approach. The former is also referred to as a basic, or theoretical approach; and the latter, as an operational, or applied approach. Aggregations of studies involving the former can be called **physical hydrology**; those involving the latter, **systems hydrology**.

In the physical approach the primary motivation is the study of physical phenomena and their understanding, while the practical application of this knowledge for engineering and other purposes is recognized but not explicitly required. A physical approach to determine output from a given system would normally require detailed specification of (a) system input, (b) system structure (geometry), and (c) physical laws, together with initial and boundary conditions.

Unlike detailed physical studies of each hydrological structure, the system approach is motivated by the need to establish workable relationship between measured parameters in the hydrological cycle to be used in solving practical technological problems. This approach generally hold that the vast complexity of the system involved in hydrological studies, the inadequacy of the available knowledge, and the knowledge likely to exist in the foreseeable future, make the possibility of a full physical synthesis so complicated that it must be discarded for practical purposes. Under these premises, a logical approach would consist of measuring those observed variables in the hydrologic cycle, which appear significant to the problem, and then attempt to establish explicit algebraic relationships between them. It is hoped that these relationships hold true within the range of conditions.

In this paper we investigate three hydrological systems in the Upper Catchments of the Jordan River (UCJR) and Lake Kinneret (LK, also known as the Sea of Galilee), Israel, for the explicit purpose of establishing an input-output relationship that can be used for reconstructing past events

or prediction of future events. However, in our approach we are concerned not only with the system operation, but also, to some extent, with the nature of the system itself (its components, their connection with one another, and so on) and the major physical laws that govern its operation. Thus our intent is to solve practical hydrological problems, and gain some physical knowledge about the hydrological systems we deal with, but at the same time to avoid the difficulties and complexity of the full physical approach.

In all three cases, the physical laws and the nature of the system are combined into a single concept of system operation. It is this concept that constitutes a so-called **gray-box**, the intermediate concept between detailed physical analysis, and the classic system approach, usually referred to as **black box**.

A system analysis model is usually expressed as (Fig. 1).

$$y(t) = \Phi[x(t)]. \qquad (1$$

Here y(t) is the model output, x(t) is the model input and the system operation Φ(x) represents a set of equations which transfer the input to the output. The problems associated with hydrological systems can be broadly classified into three types (Fig. 1, Singh 1988): 1. In the **prediction** problem the input x(t) and the system Φ(x) are known, while the output y(t) should be predicted; 2. In the **identification** problem both the input x(t) and the output y(t) are known, but the equations and parameters that describe the system Φ(x) should be identified; and 3. In the **detection** problem, the output y(t) and the system Φ(x) are known, and the objective is to detect the input x(t). The first type is referred to as a **direct problem** while the other two are known as **inverse problems**. Each of the three hydrological problems that we show here will exemplify one of these three categories, applied for practical purposes to the region of the UCJR and LK.

Study area

The UCJR, located in the central part of the Jordan Rift Valley (Northern Israel, Fig. 2a), is the most important surface water resource in Israel, providing approximately 35% of its annual drinking

water, a proportion that is constantly increasing. The area of the drainage basin of the UCJR and its tributaries is ~1700 km^2, where ~920 km^2 are in Israel, and the rest of the area is in Syria and Lebanon. The UCJR is the major water source of LK, while the other sources of LK originate from the direct watershed, located in the immediate vicinity of the lake (Fig. 2b). The direct watershed area is ~1,100 km^2, where 750 km^2 are the southern part of the Golan Height in the east of the lake, and the other 350 km^2 are part of the Eastern Galilee Mountains in the west of LK. The lake is heavily deployed and supplies ~30% of the water in Israel through the National Water Carrier (NWC). The average area of the lake surface is 166 km^2, the average volume is 4,100 Mm^3, and the average residence time is ~8.3 years.

The objective of this paper is to show how system hydrology studies were applied to three major hydrological problems of the region (Table 1): 1. **Identify** the hydrological system of the Jordan River sources (based on Rimmer and Salingar 2006); 2. **Detection** of three important components of the monthly water-solute-heat balances of LK (Assouline 1993; Rimmer and Gal 2003), and 3. Long-term **predictions** of LK salinity in response to operational changes (Rimmer 2003).

2. KARST HYDROLOGICAL SYSTEM OF THE HERMON MOUNTAIN

Description of the problem

In karst basin part of the water from precipitation may enter the earth surface through high permeability channels and voids that feeds the karst network (preferential flow), and may produce quick and large response of groundwater discharge to rainfall events. Other part may infiltrate through low permeability areas to the soil, and contribute smaller changes to the groundwater level (Jeannin and Grasso 1997). In addition, typical for karst regions, large springs may immerge into streams in various locations and contribute large baseflow, which is not related to the size of the geographic surface catchments.

Some of these characteristics are typical to the hydrology of the three major sources of the UCJR located in the south of the Mt. Hermon Range in northern Israel (Fig. 2c). Mt. Hermon is an

elongated, 55 km long and 25 km wide anticline of mostly karstic limestone of the Jurassic age with thickness >2000 m. Only seven percent of the range lies in Israel while the rest is divided equally between Syria and Lebanon. The range is the highest mountain range in Israel. The summit, 2814 meters above sea level (ASL), is in Syria. The Hermon high regions (above 1000 m ASL) receive the most precipitation in Israel (>1300 mm $year^{-1}$), restricted to the wet season from October to April. Snow usually falls on the elevated areas from December to March, and persists on areas above 1400–1900 m ASL (Depending on local conditions) until March–June. Rainfall and snowmelt of Mt. Hermon recharge the main tributaries of the UCJR: (1) Dan (255×10^6 m^3 annually), (2) Snir also known as Hatzbani (118×10^6 m^3) and (3) Hermon also known as Banyas (107×10^6 m^3) (Fig. 3).

Because of the sensitivity of water resources for the entire region (including Syria and Lebanon), and the requirement to keep the status quo, the Hermon region did not undergo anthropogenic changes during the last decades compared to other major hydrological systems in Israel. For example, no significant land use changes or pumping were made in the entire Mt. Hermon area. Despite the great importance of this mountainous area, only few hydrological quantitative studies were conducted (Simpson and Carmi 1983; Gilad and Bonne 1990; Gur et al. 2003). The geological settings of the southern region of Mt. Hermon was partly described in the past (Michelson 1979), however, apart from the delineation of the location of the Jurassic exposures (Fig. 2c) which contribute to the knowledge about the extension of the karstic region, and some geological cross sections (Gilad and Schwartz 1978), the knowledge about the geohydrology of the region is practically limited. The lack of hydrological data is typical to Mt. Hermon, and include the following:

a. The amount of snow and rainfall on Mt. Hermon, was never measured systematically because of the difficulties in maintenance of meteorological station at altitude above 2,000 m ASL. Hence estimations of snow and rainfall in previous studies were based on stations located at lower elevations (Gilad and Schwartz, 1978; Simpson and Carmi, 1983).

b. A complete water balance for the region is difficult to compute because the stream and springs flow in the east and northeast region of Mt. Hermon is in Syria and Lebanon, and there is no hydrological data sharing between Israel, Syria and Lebanon.

c. The thickness and the borders of the aquifer(s), water level fluctuations, hydraulic characteristics (i.e., conductivity, porosity), and the local rainfall distribution, are unknown.

d. The well-developed karstic landscape causes large preferential flow into groundwater and relatively little surface runoff. These types of flow increase the complexity of quantitative studies.

e. Finally, the location of different aquifers in the region, and the recharge area of the three main tributaries of the Jordan River are unknown. Moreover, recharge areas are not correlated with the size of the geographic surface water catchments.

In contrast to considerable lack of information from Mt. Hermon area, there is an excellent database on the hydrology of the Jordan River, south from Mt. Hermon. It includes long-term stream flow data, daily rainfall, daily pan evaporation measurements, monthly water consumption, and more.

System type and objective

The existing data types and the lack of others, call for a system analysis model (Eq. 1). In this case the model input x(t) is long-term time series of extrapolated daily precipitation and evaporation; the output y(t) is long-term predictions of daily stream flow, which can be calibrated versus the measured data; and the unknown is the system operation $\Phi(x)$, representing a set of equations which transfer precipitation to streamflow. The problem of recognizing the main temporal and spatial characteristics of the Mt. Hermon hydrology is an **inverse problem** of the type **identification**. The objective of this study (Rimmer and Salingar 2006) was to **identify** an appropriate system model $\Phi(x)$, for both the baseflow and the surface flow components of a karst basin, and to get better quantitative understanding of Mt. Hermon hydrology. In the proposed

system special attention was given to a method to deal with the uncorrelated base and surface flow, and to the large-scale preferential flow to groundwater. The model was applied to the three main tributaries that originates from the karst region of Mt. Hermon, which forms nearly the entire flow of the Jordan River.

The system, mathematical representation and solution

The input: Long-term daily rainfall data (some started back in the beginning of the 20 century) were analyzed. We found clear indications that in northern Israel, average monthly rainfall is nearly a linear function of the elevation. However, the linearity is slightly weaker and less significant during the beginning of the winter (October), increase towards the middle of the winter (January), and gradually decreases towards the end (April). Measured daily precipitation also verified that the variations between rain gauges and the timing of maximum and minimum precipitations are similar for most rain gauges stations. A representing rainfall gauge of the entire Hermon region was therefore defined using a combination of elevations and daily rainfall from several gauging stations in the Upper Galilee and the Golan Heights. Potential evaporation estimations were based on long-term (1970-2000) daily measurements of pan A evaporation (Ponce 1989). Unlike precipitation, spatial evaporation was not calculated, because only three locations of long-term measurements were available. Mean seasonal pan evaporation trend for the UCJR was computed similarly to Viney and Sivapalan (2000). For calculating actual evaporation we used a simple estimation in which evaporation is a function of "dry days" counted from the day of the last rainfall event.

…..The output: Daily discharges of the main UCJR tributaries – Dan, Snir and Hermon - (Fig. 3) were measured (1970-2005) by continuous monitoring of the water level in the stream, and calibrated by periodic measurements of stream velocity profiles. The measured data were corrected for each stream by adding the actual consumptions upstream to the measured data. In the three measured flow time series, baseflow was separated from surface (or quick) flow and created six time series – two for each tributary. Baseflow separation parameters were performed with Eckhardt (2005) method. Results of the separation analysis (Fig. 3) were used to calibrate the model output.

…..The system main equations:

A conceptual HYdrological Model for Karst Environment (HYMKE, Rimmer and Salingar 2006) consisting of 3 surface flow catchments, and four regional phreatic aquifers, was proposed as the sources of the surface and baseflow components of the entire region.

HYMKE is made of 4 modules (Fig. 4): the surface layer (0), the vadose zone (1), groundwater (2) and surface flow (3). In the conceptual model the earth surface of the entire geographical basin is recharged by precipitation, and dried by evaporation, surface runoff and percolation to deeper layers. The karst nature of the landscape was introduced similarly to Jeannin and Grasso (1997), with a surface layer ("epikarst") composed of low permeability section, and high permeability section that feeds the karst network. The surface layer is drained continuously as a function of moisture content. Saturation excess is generated when the surface layer is saturated, and then, part of the excess saturation is transformed into surface flow (module 3), while the other part forms a downward preferential flow component. Therefore, the percolation into the vadose zone (module 1) includes both "slow flow", i.e., Darcy flow that depends on the soil moisture content and hydraulic conductivity, and "quick flow" which is effective mainly during the peak of the wet season. The output from the vadose zone (module 1) feed the groundwater reservoir (module 2). However, the differences between the groundwater discharge patterns require the separation of module 2 into several groundwater reservoirs. In the case of Mt. Hermon these are the 3 reservoirs feeding the Dan, Snir and Hermon baseflow component, and one reservoir that contribute the residual of groundwater to springs in the east part of Mt. Hermon in the area of Syria. Combining the output of the surface runoff module (3) and the baseflow module (2) for each stream result in the full natural flow of each tributary. The sum of all three tributaries will create the flow in the main stream, the Jordan River.

The module 0 of the surface layer is governed by the mass balance equations:

$$\theta_j = \begin{cases} \theta_{Pj} & ;\text{if } (\theta_{Pj} < \theta_S) \\ \theta_S & ;\text{if } (\theta_{Pj} >= \theta_S) \end{cases} \qquad \text{(2.1}$$

$$\text{where } \theta_{Pj} = \theta_{j-1} + \frac{q_{IN_j} - q_{OUT_j}}{\Delta z}$$

Here θ is the moisture content ($m^3\ m^{-3}$), θ_P the "potential" moisture content, θ_S indicate saturation, Δz the thickness of the topsoil layer (m), and 'j' is the daily index. The daily flux into the surface layer $q_{IN\,j}$ (m) was defined as:

$$q_{IN_j} = 0.001(R_j - E_{A\,j}) \qquad \text{(2.2}$$

where R_j and $E_{A\ j}$ are the daily rainfall and daily evaporation time series in mm (see input description above), and the 0.001 originates from changing units (mm to m). We assumed that the daily moisture of the surface soil to a depth Δz is uniformly wet. Under this condition, q_{OUT} was described with the "unit gradient" assumption, in which the vertical flux, defined by Darcy law is reduced to:

$$q_{OUT\,j} = -K_D(\theta_j) \qquad \text{(2.3}$$

Here $K_D(\theta)$, the unsaturated hydraulic conductivity of the soil (m day^{-1}), is a well known function of the soil moisture content θ (Mualem and Dagan, 1976). Note that while the θ is set on θ_S, the difference θ_P- θ_S in Eq. 2.1 is the excess saturation. We propose that only constant part of this component ($0 \le \alpha_{Sk} \le 1$) is contributed to surface runoff Q_S, and the residual, Q_{PR}, flows downward as preferential flow, typical for karst environment. The excess saturation (10^3 m^3) is therefore represented by:

$$Q_{Sk}(t) = A_k \alpha_{Sk} [1000 \times \Delta z \times (\theta_P(t) - \theta_S)] \qquad \text{(2.4}$$

and

$$Q_{PRk}(t) = A_k (1 - \alpha_{Sk}) [1000 \times \Delta z \times (\theta_P(t) - \theta_S)] \qquad \text{(2.5}$$

Here A_k is the surface area (km^2) of the k's tributary (k=1,2,3), and α_{Sk} can be calibrated versus measured surface flow.

The next modules (1, 2 and 3 in Fig. 4) are combinations of linear reservoirs. A linear reservoir has an outflow proportional to the amount of water stored in it. The theory of linear reservoir is often used in surface and groundwater hydrology as models for the management and control of inflows and outflows in water reservoirs (Singh 1988; Sugawara 1995). The equations for a continuous water balance in linear reservoirs are:

$$\frac{dh(t)}{dt} = \frac{Q_{IN}(t)}{A} - \frac{h(t)}{K} \quad \text{s.t.:} \quad h(0) = \frac{KQ_{OUT}(0)}{A} \qquad (2.6$$

where h(t) (mm) is the height of the water level in the reservoir above the outlet, A (km^2) is the reservoir area, Q_{IN} and Q_{OUT} (10^3 $m^3 \times day^{-1}$) the inflow and outflow respectively, and K (to distinguish from K_D) is a storage coefficient with the dimension of time (day).

If $Q_{IN}(t)$, and the coefficients A and K are known, and the initial condition is prescribed by a measured flow $Q_{OUT}(0)$, then Eq. (2.6) can be solved numerically or analytically for h(t), and the outflow $Q_{OUT}(t)$ can than be calculated with:

$$Q_{OUT}(t) = \frac{Ah(t)}{K} \qquad (2.7$$

The surface flow module (3) takes as input part of the daily pulse of excess saturation (Q_{Sk} in Eq. 2.4) and transforms it into the stream flow by a simple linear reservoir operator (Eq. 2.6). The output (Eq. 2.7) represents the surface flow for each tributary and calibrated against the surface component of the separation analysis. The vadose zone module (1) takes as input the other part of the daily pulse of excess saturation (Q_{PRk} in Eq. 2.5) and the Darcian flow component (q_{OUT} in Eq. 2.3), and transforms them into an input to the groundwater reservoirs. The groundwater module (2) takes as input the output of module 1, and transforms it into the baseflow. This groundwater output represents the calculated baseflow for each tributary and calibrated against the baseflow from the separation analysis.

Results and discussion

The full model (modules 0, 1, 2 and 3) was tested by reconstruction of both the surface and baseflow during a continuous period from 01 Jan 1986 to 30 Sep. 2000, and then was verified by applying the calibrated parameters to the periods 01 Jan 1970 to 31 Dec 1985 and 01 Oct 2000 to 30 Sep 2004.

Input data includes single time series of daily precipitation that retain both the daily trends of the rainfall in the region and the extrapolated average monthly precipitation of Mt. Hermon. The model did not take into account the type of precipitation (rainfall, snow) because of the lack of information. We also applied the best estimations of potential evaporation, but the parameters of the real evaporation had to be calibrated.

Calibration of the surface layer and the surface flow was based on accurate simulation of the days when saturation occurred and excess saturation caused surface flow. The calibrated parameters resulted in correlations of r^2=0.60 and r^2=0.75 between the calculated and the separated surface flow of the Snir and Hermon streams, respectively (Fig. 5), while the contribution of surface flow to the Dan was negligible. Model predictions of surface flow were less successful in days of extreme events. This is probably due to the lack of data about snow melting, the crude assumptions on which the "surface layer" module was based, and especially the assumption of constant division between surface runoff and preferential flow. However, the calibration of these modules may be improved by adding more procedures and parameters.

After calibration of the surface modules was completed, the linear reservoir (Eq. 2.6) of module 2 was solved numerically for $h_1(t)$, using the Runge-Kutta method, with the downward flow and preferential flow from the surface layer as input. The outflow from the reservoir was calculated with Eq. (2.7), and the values of the constants α_{Bk} were calibrated to fit the contribution to each groundwater reservoir $Q_{IN2\ k}(t)$ separately. Then, Eq. (2.6) was solved numerically for $h_{2\ k}(t)$, using the same method, and Eq. (2.7) was used to calculate the baseflow of each tributary (Fig. 6). The calibrated parameters of these two modules resulted in correlations of r^2 = [0.84, 0.89, 0.77] and

Nash-Sutcliffe coefficient (NC) = [0.71, 0.80, 0.21] between the calculated and the separated base flow of the Snir, Hermon and Dan streams, respectively. Figures 7 and 8 show the final steps of the modeling process. In Fig. 7 the sum of calculated baseflow and surface flow is compared to the FNF of each of the three tributaries, while Fig. 8 shows the results for the flow in the Jordan River with r^2 = 0.94 and NC=0.79 for the same period.

Our approach for a primary, but systematic mass balance was based on setting the parameter A_1 on the cumulative area of the three surface catchments Dan, Snir and Hermon (A_1=783 km^2). This is a reference point, which enables systematic definitions of mass balance. We calculated the representing annual precipitation of the entire Hermon region as ~958 mm. Altogether the entire annual precipitation is equivalent to 783 km^2 multiplied by 0.958 m of rainfall, which result in 750 million m^3 (Mm^3). The total calculated potential evaporation was ~1900 mm, but if the altitude is taken into account this value may be reduced to 1000-1200 mm annually (according to National Action Programme, Chapter Two: Environmental Status in Lebanon, http://www.codel-lb.org/Chapter%20II.pdf). Real evaporation in the model was 226 mm (~177 Mm^3); the calibrated surface flow is only 90 mm (70 Mm^3, compared to 83 Mm^3 from separation); the calculated downward flux includes 275 mm (215 Mm^3) from Darcian flow and 367 mm (287 Mm^3) from preferential flow, which sums up to 502 Mm^3 according to the model, and 393 Mm^3 according to the measured data. The ~109 Mm^3 difference is probably contributed to the east part of Mt. Hermon, such as the Beit Jinn and Sabarani springs in Syria, as was actually suggested by Gur et al. (2003) and others.

Current use of the system

The Israeli Hydrological Service, decided recently to use HYMKE as a decision making tool, which will be operated parallel to other types of models. The model was applied successfully to another karst system (LK regional aquifers). It is now under continuous process of improvements.

3. THE SYSTEM OF MONTHLY WATER-SOLUTE-HEAT BALANCES OF LAKE KINNERET

Description of the problem

Water, solutes and heat budgets are a common procedure applied on a routine basis to sources of water, and especially to lakes, in order to determine available water, rainfall-discharge relationship, evaporation estimation, lake-groundwater relationship and water quality issues. The results of continuous, long term, periodic budgets are essential in order to study the hydrological system of the lake and to determine a long-term operational policy.

Annual publication on the monthly water, solute and heat balances of LK have been carried out and reported on a regular basis by Tahal (Water Planning for Israel Ltd.) from 1950's and more accurately from1963 to 1986. Since 1987, Mekorot (Israel National Water Co.) conducted the balances annually. While Tahal separated the solute from the water and heat calculations, according to the Mekorot method (Assouline 1993), all three balances were calculated simultaneously every month. In this procedure, measured properties of the three balances, which are monitored continuously on a monthly (or biweekly) basis, were used to calculate the closing residuals of the balances. The entire procedure is completed for each month when all three equations (i.e., water solute and heat) are balanced, and the residual of each equation is found and evaluated.

In LK, two essential variables for lake management - the evaporation (Assouline and Mahrer 1993), and the unknown inflows of water and solutes from the saline springs (Rimmer and Gal 2003) - are calculated from the balances. Annual evaporation losses in LK are relatively high (270 ± 30 million m^3 annually or ~1600 mm, Rimmer et al. 2006), about 36% of the mean annual outflows from the lake. During dry years, when pumping is reduced, evaporation rates can reach ~50% of annual outflows. The annual mean discharge from the saline springs was approximated as ~78 Mm^3 (only 10% of the water inflows) with an average salinity of 1,160 mg L^{-1} and an average a

temperature of 27^{o}_{C}. The annual solute discharge was $78\times1,160=90,480\times10^{6}$ kg Cl^{-}, or $7,540\times10^{6}$ kg Cl^{-} monthly (nearly 90% of the entire solute inflows to the lake).

System type and objective

In this system the model output y(t) is a monthly summation of all the measured variables from the water, solute and heat balance. It includes all measured inflows and outflows, and the measured monthly differences between storage of water, solute and heat in the lake. The input x(t) includes three unknowns: the saline springs inflows, the salinity of the these springs, and the evaporation. The system operation $\Phi(x)$ represents a well known (Winter 1981; Assouline 1993) set of physical equations and assumptions which transfer the input to the output. This case is an **inverse problem** of the type **detection**, where we look for the unknown input. The objective here is to calculate systematically the three unknowns of the monthly balances. An important aspect of lake budgets is the effect of uncertainty related to the measured and evaluated components involved (Winter 1981). This issue was discussed in details by Assouline (1993), Rimmer and Gal (2003) and Rimmer et al. (2006), but will not be part of this contribution.

The long-term analysis is essential in particular to define the functional relationship between the periodic changes of water levels in the lake and the discharge from the saline springs (Mero and Simon 1992; Rimmer and Gal 2003).

Mathematical representation and solution

When measured values are separated from unknowns (Figure 9), the water balance equation of LK is:

$$Q_{ur} + Q_s - Q_e = \Delta V_L + Q_d + Q_p - Q_{gs} - Q_j - Q_y - Q_r - Q_{mr} \qquad (3.1$$

where the monthly measured quantities (Mm^3) at the right hand side of eq. 3.1 are ΔV_L the change in water volume of the lake, Q_d release through the Degania dam, Q_p withdrawal of water by pumping to the National Water Carier (NWC) and by private consumers, Q_j the Jordan River discharge, Q_y water diverted to the lake from the Yarmuch River, Q_r Direct rain, Q_{mr} runoff from

the gauged part of the direct watershed, and Q_{gs} discharge from the gauged part of the saline springs. The monthly-unknown quantities (Mm^3) at the left hand side of Eq. 3.1 are evaporation loss, Q_e, the unmonitored saline springs contribution, Q_s, and runoff from the ungauged direct watershed Q_{ur}.

Using the same procedure for the heat balance of LK result in the equation:

$$T_{ur}Q_{ur} + T_sQ_s - KQ_e = \Delta H_L + \sum_i T_iQ_i - R_n \qquad (3.2$$

$$K = L(1+\beta)+T_0$$

where R_n Net radiation at the surface, ΔH_L the change in heat storage in the lake, T_i the respective monthly mean temperature of the i-th measured component (i- subscript index), L, latent heat of water, T_0 the water surface temperature and β Bowen Ratio. In terms of eq. 3.1 and assuming that rainfall and water vapor are salt free, the salt balance equation is

$$C_{ur}Q_{ur} + C_sQ_s = \Delta S_L + \sum_i C_iQ_i \qquad (3.3$$

where ΔS_L the change in salt storage in the lake and C_i the respective monthly mean chloride concentration of the i-th measured component (i- subscript index).

Denoting by W (for water), H (for heat), and S (for salt) the results from the operations on the measured components as they are expressed in the right hand side of eqs. 3.1,2,3 the expression of the system of equations to be solved is:

$$\begin{bmatrix} 1 & 1 & -1 \\ C_{ur} & C_s & 0 \\ T_{ur} & T_s & -K \end{bmatrix} \begin{bmatrix} Q_{ur} \\ Q_s \\ Q_e \end{bmatrix} = \begin{bmatrix} W \\ S \\ H \end{bmatrix} \qquad (3.4$$

Equation 3.4 could not be solved without further assumptions. First, Based on occasional measurements during floods in the ungauged basins, C_{ur} and T_{ur} are assumed to be practically equal to the measured C_{mr} and T_{mr}; second, Q_{ur} was evaluated (and denoted by Q_{ur}^*) by assuming a simple proportion between runoff fluxes from neighboring gauged and ungauged watersheds; and third, a linear relationship between C_s and T_s was fitted (Mero 1978). Under these 3 assumptions, the

system in 3.4 becomes:

$$\begin{bmatrix} 1 & -1 \\ C_s & 0 \\ f(C_s) & -K \end{bmatrix} \begin{bmatrix} Q_s \\ Q_e \end{bmatrix} = \begin{bmatrix} W - C_{ur}^* \\ S - C_{ur} Q_{ur}^* \\ H - T_{ur} Q_{ur}^* \end{bmatrix} \quad (3.5$$

Equation 3.5 holds three unknowns inputs: Q_e, Q_s and C_s and therefore it has a unique solution. If a linear relationship between C_s and T_s is presented:

$$f(C_s) = T_s = aC_s + b, \quad (3.6$$

the solution of 3.5 leads to the evaluation of the three detected inflow variables.

$$Q_e = \frac{(H - T_{ur} Q_{ur}^*) - a(S - C_{ur} Q_{ur}^*) - b(W - Q_{ur}^*)}{b - K}; \quad Q_s = W - Q_{ur}^* + Q_e; \quad C_s = \frac{S - C_{ur} Q_{ur}^*}{Q_s} \quad (3.7$$

Results and discussion

Solution of equation 3.6 results in the monthly evaporation from the lake (Q_e), the monthly inflows of the saline springs (Q_s), and the average monthly salinity (C_s) of the entire inflows of the springs. The entire process can be repeated from one month to another to create the time series that complete all three mass balances. With this procedure, the mean annual evaporation for 1968-2002 was calculated as ~1,450±130 mm, with maximal evaporation during July (>185 mm) and minimum during February (<50 mm) (Fig. 10).

While the calculated evaporation is easy to approximate with the water and energy balances method, the solution of the other two variables in equation 3.7 (Q_s and C_s) often results in non-physical values such as negative spring flow discharges (Fig 10), and/or negative, or extremely high values of spring salinities, caused by the noise in the calculated S time series. In order to minimize the effect of noise, it is proposed to solve the mass balances equations with the following procedures (Rimmer and Gal 2003): First, it is essential to solve the problem with as long time series of W, S, and H as possible; second, it is recommended to replace the time series S with a smoothed series, S^* which contain only few negative values and which is much more stable then the original S_k series. Third, it was found that if a constant C_s=~1,160 mg L^{-1} was assumed there was a

good closing of the entire lake mass balances. Note that according to the typical salinity-temperature relations of the Kinneret saline springs (Equation 3.6) $T_s=0.002\times C_s+25.1$ (T_s is the temperature), the salinity of $C_s\cong 1{,}160$ mg L^{-1} is equivalent to a temperature of 27^oC. Using the temperature of 27^oC for the entire saline springs discharge in a one-dimensional LK energy model (DYRESM) over 10 years, resulted in the best estimation of the lake temperature (Gal pers. com.).

The time series that complete the water, solute and energy balances are demonstrated in Fig. 10. The results were used to clarify issues of the salinization mechanism, which were under debate for several decades. We found a positive relation for both water and solute discharges of the saline springs with lake levels, i.e., there were high fluxes of ground water, and high leaching of solute during rainy winters, indicating that the major salinization mechanism of the lake is leaching of brines by groundwater (Gvirtzman et al 1997; Rimmer and Gal 2003). In addition, we examined the monthly solute flux against the monthly water discharge. We found that the solute mass increases with the water discharge, in agreement with the conclusions of Moshe (1978) and Benoualid and Ben-Zvi (1981), but in contrast with model results reported by Simon and Mero (1992). We also show that there is a positive relationship between annual solute influx and annual depth of precipitation, and therefore concluded that rainy winters cause higher fluxes of the groundwater to the lake, and higher quantities of solute, a conclusion, which brought an important understanding to the dispute on LK salinization mechanism (Goldschmidt et al. 1967, Mero and Mandel 1963; Gvirtzman et al 1997).

Current use of the system

The water-heat-solute balances system is continuously used by the Watershed Unit of Mekorot (1987 till today) to calculate and publish the annual summary of changes in LK hydrological variables.

4. THE SYSTEM OF LAKE KINNERET SALINITY

Description of the problem

Increased lake salinity is a growing problem in arid and semi arid regions. Operational management, which is based on a reliable hydrological understanding, has the potential to control the lake salinity. This is the case of LK, where saline water flows into the lake through on-shore and off-shore springs, causing the salinity of the lake to be relatively high (180-300 ppm Cl^-). The history of LK salinity is documented since the beginning of the 20-th century (Dalinsky, 1969). In 1964, the Israeli National Water Carrier (NWC) became operative, and the chloride content began to drop from ~390 ppm Cl^- (Figure 11); this trend was enhanced in January 1965, when the Saline Water Carrier (SWC, a canal that diverts the north-western shoreline saline springs from the lake) was fully operated. Lake salinity dropped significantly between 1965 and 1968, and was further enhanced by the exceptional winter of 1968-69 (inflows of 200% compared to an average year). The lowest lake salinity, 192 ppm Cl^-, was reported in May 1988. It then increased to 250 ppm Cl^- following three dry winters, and decreased to ~210 ppm Cl^- following the exceptionally rainy winter of 1991-1992. From the end of the winter 1993-1994 to the winter of 2001-2002, the annual average lake salinity has increased and the annual average lake level has decreased constantly.

The most significant variable in the analysis of LK salinity is the solute mass inflow to the lake. Ben-Zvi and Benoualid (1981) calculated the annual average total inflow of solute to the lake as 161×10^6 kg for the period 1960-1979. Simon and Mero (1992) calculated an average of 159.4×10^6 kg×year^{-1} for the period 1960-1986, with a standard deviation of 18.7×10^6 kg×year^{-1}. Rimmer (1996) calculated the solute mass inflows to the lake for the years 1968-1996 in four groups: 1. The springs diverted by the SWC (~38×10^6 kg×year^{-1} from Tabgha and ~17×10^6 kg×year^{-1} from Tiberias); 2. the measured springs that flow to the lake (~12×10^6 kg×year^{-1}); 3. The unknown springs (~78×10^6 kg×year^{-1}); and the surface flow contribution (~15×10^6 kg×year^{-1}). His annual average solute inflow (~160×10^6 kg×year^{-1}) was in agreement with previous estimations.

Several policies for the operation of the lake were examined in the past using models to predict the expected lake salinity changes. F. Mero developed in the late 70's a model for the effect of operational aspects such as pumping and saline springs diversion (Mero and Simon, 1992). Ben-Zvi and Benoualid (1981) developed a model, which connected between the semi-annual solute inflow, water discharge and rainfall. Assouline et al. (1994) suggested a monthly-based model for the same purpose. Berger (2000) further developed Assouline's model into a general operational model for the LK system. All the proposed models were lake-wide numerical models, based on statistical analysis of data of water discharge to the lake, and solute discharge from the saline springs system.

The proposed system approach model is a lake-wide model for the salinization mechanism, based on the main components of the solute balance. However, unlike previous statistical models, it proposes that with the appropriate assumptions LK salinization mechanism can be described by a simple physically based model (complete mixing) and therefore can be solved analytically. The solution allows us to easily examine the influence of each component of the solute balance on the expected salinity changes. Predictions of the lake salinity changes were demonstrated for the cases of controlled increase or decrease of saline springs discharge to the lake, and for the changes of water quantity allowed to flow into or pumped out of the lake.

System type and objective

The **input** data x(t) of this hydrological system represent long-term annual stream inflows, outflows, and evaporation, direct annual rainfall, and average stream salinity; the **system operation** $\Phi(x)$ represents the equations of complete mixing (CM). The theory of CM is often used in geochemical analysis of water resources (Lerman, 1979; Varekamp1988). In a CM model, solute flux through the outlet is proportional with solute storage (Fig. 12). The **output** y(t) is the long-term predictions of solute mass and volume of the lake, based on the input. This problem exemplifies the **direct problem** of **prediction**.

The objective of this work was to verify an existing well-known physical mechanism, and to use it as a tool to predict long-term changes of chloride concentration in the lake. The theoretical mechanism was tested against special cases of long-term salinity changes in LK in the past, and then was used to predict the long-term influence of future operation policies on lake salinity.

Mathematical representation and solution

The equation for the continuous water balance in the lake is:

$$\frac{dV(t)}{dt} = Q_{in}(t) - Q_{out}(t) \qquad (4.1$$

where V is the volume of the lake (Mm^3); t is time (year); Q_{in} ($Mm^3 \times year^{-1}$) the inflow discharge; and Q_{out} the outflows ($Mm^3 \times year^{-1}$). Similar to the water, the solute balance of the lake can be written as:

$$\frac{dS(t)}{dt} = S_{in}(t) - S_{out}(t) \qquad (4.2$$

Where $S = C_{lake}V$ is the solute mass in the lake (kg), represented by multiplying the average chloride concentration C_{lake} (ppm Cl^-) by the lake volume V (Mm^3); S_{in} is the incoming solute flux ($kg \times year^{-1}$); and S_{out} is the solute outflow flux ($kg \times year^{-1}$) through pumping and water release.

The incoming solute flux, S_{in} (Eq. 4.2), may be written as a product of total water flux Q_{in} and a single, averaged solute concentration, $\overline{C}_{in}$:

$$S_{in}(t) = Q_{in}(t)\overline{C}_{in}(t); \quad Q_{in} = \sum_i Q_i ; \quad \overline{C}_{in} = \frac{\sum_i Q_i C_i}{\sum_i Q_i} \qquad (4.3$$

where i is the index of inflow sources. It is assumed that a mechanism of complete mixing can be applied to the lake, and therefore the concentration of solutes in the outflows is equal to the average lake salinity, i.e.:

$$S_{out}(t) = Q_{out}(t)C_{lake}(t) \quad ; \quad C_{lake}(t) = \frac{S(t)}{V(t)} \qquad (4.4$$

Substituting equations 4.3 and 4.4 into equation 4.2 results in:

$$\frac{dS(t)}{dt} = Q_{in}(t)\overline{C}_{in}(t) - \frac{Q_{out}(t)}{V(t)}S(t) \qquad (4.5$$

Eq. 4.5 may be written in the form:

$$\frac{dS(t)}{dt} + q(t)S(t) = S_{in}(t) \quad ; \quad s.t.: S|_{t=0} = S_0$$
$$q(t) = \frac{Q_{out}(t)}{V(t)} \quad ; \quad S_{in}(t) = Q_{in}(t)\overline{C}_{in}(t) \qquad (4.6$$

The S_0 in Eq. 4.6 represents the initial solute mass in the lake, and q stands for the ratio of outflows to lake volume, which is the water renewal rate, or the reciprocal of water residence time (Wetzel, 1983). Assuming a constant long-term operation policy within the computational time period, with constant outflows, inflows and a steady lake level (i.e. q and S_{in} are constants), the solution of Eq. 4.6 is then given by:

$$S(t) = \frac{S_{in}}{q} + \left(S_0 - \frac{S_{in}}{q}\right)\exp(-qt) \qquad (4.7$$

The expression $(S_0 - S_{in}/q)$ is the lake system full response to changes in solute and/or water inflows and outflows. If this expression is zero, lake solute mass remain constant; if the expression is negative, lake solute mass increase, and vice versa. We are particularly interested in the solution of equation 4.6 over periods in which S_{in} (representing the degree of control, and the natural fluctuations of the saline springs inflows,) and q (representing policy of pumping, and overflow from the lake) change in steps (i=0…n) from one period to another. For this type of step changes we can also use the solution of 4.7 as explained by Rimmer (2003).

Results and discussion

This system was tested and verified mainly for the years 1964-2000, as the LK salinity data for this period are more reliable than data from previous years. Moreover, monthly water and solutes balances of the lake (Water Planning for Israel, 1968-1986; Mekorot, 1987-2005, see above) support the reliability of these data.

Steady state: Mean annual net inflow (total inflow, including direct rainfall-evaporation) of

water for the entire period was 490 Mm^3; mean annual outflows (not including evaporation) were 498 Mm^3; and mean lake volume was 4,020 Mm^3. The time to reach steady state of the lake salinity can be estimated by calculating the mean q. Applying the calculated mean $\overline{q} = 0.12$ (residence time $=1/\overline{q}=8.3$ years) to Eq. 4.7 result in a change of 70% in the system response during the first 10 years, and a change of 91% of the system response during the first 20 years. A steady state can therefore be considered after nearly 3/q (~25) years. By then the solution in Eq. 4.7 nearly reduces to the expression $S(t) = S_{in}/q$. Taking for example $S_{in}=160\times10^6$ kg×year^{-1} as the annual mean solute inflow to the lake without the diversion of the SWC (Simon and Mero 1992), and using q=0.12, the calculated solute mass in the lake at steady state was ~$1{,}333\times10^6$kg, and the calculated salinity (with V=4,020 Mm^3) was ~330 ppm Cl^-, similar to the average measured values prior to 1960. As a result of the operation of the SWC, which diverts an average of ~55×10^6 kg×year^{-1} from the lake, the average annual inflows was reduced to $S_{in}\cong105\times10^6$ kg×year^{-1}. The calculated solute mass in the lake for steady state is then ~875×10^6kg, and the expected calculated salinity is ~218 ppm Cl^-. Similar values were measured in the lake since 1980 (Figure 11).

Lake salinity changes in time: The most obvious example of long term salinity changes is the period 1964-1987 following the operation of the SWC in 1964. This period duration is nearly 3/q years, i.e., at the end of this period lake salinity is close to reach a steady state. During these years lake solute mass decreased from $1{,}550\times10^6$ kg to 861×10^6 kg, and lake salinity decreased from 367 to 212 ppm Cl^-. The natural exponential decay of solute mass and the reduction of the salinity of the lake are illustrated in Figure 13a. Special attention needs to be drawn to the exceptionally rainy season of 1968-69. This season contributed a relatively high (~160×10^6 kg) solute mass to the lake. Nevertheless this season contributed more than twice the annual average inflows, and the value of q was 0.302 compared to an average of 0.127 for the period 1964-87. As a result, lake solute mass dropped significantly faster than the predicted exponential decay. However, on a 23 years scale the exponential decay represents well the salinity changes.

Another example is the period 1989-2000, illustrated also in Figure 13b. The annual solute balance shows an increased discharge from an average of 95×10^6 kg during the years 1970-1989, to nearly 109 $\times10^6$ kg in 1989-2000. This change was explained by the less effective usage of the SWC, and the solute inflows increase during the rainy winters of 1991-92 and 1992-93. These two reasons added together ~14×10^6 kg Cl^- to the average solute inflows at this period. In addition, lake volume varied significantly, from ~3,600 Mm^3 in 1991 to ~4200 Mm^3 in 1992 and back to 3,600 Mm^3 in 1999. Applying Eq. (7) to this period with the calculated average annual values (q=0.115; S_{in}=~109×10^6 kg) resulted in an exponential increase of the solute mass and a fairly good description of lake salinity despite all the major changes in the hydrology of the lake.

Predictions: The purpose of this section is to demonstrate the use of Eq. (4.7) to predict the long term influence of future operation policies on the lake salinity.

Change of Saline Springs Discharge: Two procedures can cause a change of the solute inflows to the lake. The direct control of solute flux can be achieved by increase or decrease of the diverted discharge into the SWC. An indirect method to change solute inflows is by increased pumping from the Eastern Galilee aquifers (Rimmer et al., 1999; Gvirtzman et al., 1997). Using the first approach, the diverted discharge can be measured directly; unlike the second approach in which the effect on the saline springs system can be evaluated only by the calculations of lake solute balance. In the following it is assumed that the average S_{in} can be controlled.

Prediction of salinity changes as a result of changes in the diverted amount is straightforward: First, the starting year t_0 and the appropriate initial lake solute mass S_0 were determined; second, a new solute inflow S_{in} was calculated; third, the mean q value of the lake was determined for a given lake level and cumulative outflows; forth, Eq. (4.7) was applied for the future years; and finally the approximated solute mass was divided by the lake volume, V. The calculated results for this procedure, with C_{lake0}=280 ppmCl^-, and Q_{out}=500 Mm^3, were plotted on the same axes for two lake levels (V=3600, 4020 Mm^3); and five solute discharges S_{in}=[70,90,110,130,140]$\times10^6$ kg (Figure 14a). The parameters of this predictions are therefore q=[0.138, 0.124] and S_0=[1008, 1125.6]$\times10^6$

kg for V=3,600, and V=4,020 Mm^3, respectively. The predictions for 10 years are a decrease of lake salinity to ~180 ppm Cl^- for $S_{in}=70\times10^6$ kg and no decrease for $S_{in}=140\times10^6$ kg. It is shown that the reduction in lake salinity for the same S_{in} is faster for lower volume, because the leaching effect on the solute mass, determined by q, is higher when lake volume is smaller.

Change of inflows from the Jordan River: Significant variations in the salinity of LK are expected also as a result of changes in the average quantity of inflows from the Jordan River and the streams from the LK direct watershed. The results for 20 years predictions for the case of reduced water inflows and outflows, with C_{lake0}=230 ppmCl^-; V=4,020 Mm^3 ($S_0=924.6\times10^6$ kg) and $S_{in}=115\times10^6$ kg were calculated for four average outflows Q_{out}=[200, 300, 400, 500] Mm^3. The q values are therefore 0.049, 0.074, 0.099 and 0.124, respectively. A significant change of lake salinity is expected as a result of the decrease of q, explaining the increase of salinity of the lake in dry seasons, and the desalinization of the lake during very rainy seasons.

Current use of the system

The above CM approach was used to explain a long term increase of salinity in Lake Biwa, Japan. The system is now improved and includes stochastic components (Rimmer et al. 2006). It is planed to be applied by the Israeli Hydrological Service for a long term salinity predictions of LK.

References

Amorocho, J., and W.E. Hart 1964, A critique of current methods of hydrologic systems investigation, Eos Trans. AGU, 45, 307– 321.

Assouline, S., 1993. Estimation of lake hydrologic budget terms using the simultaneous solution of water, heat, and salt balances and a Kalman filtering approach - application to Lake Kinneret. Water Resources Research, 29(9): 3041-3048.

Assouline, S. and Y. Mahrer.1993: Evaporation from Lake Kinneret 1. Eddy Correlation System Measurements and Energy Budget Estimates. Water Resources Research. 29, (4):901-910.

Assouline, S., Shaw M., Rom M., 1994. Modeling the solute and water components in Lake Kinneret System. WaterShed Unit, Mekorot, Sapir Site, Israel. (in Hebrew).

Ben-Zvi, A., Benoualid, S. 1981. A model to predict the Lake Kinneret salinization and the solutes storage. Israel Hydrological Service report 1981/5 (in Hebrew).

Berger, D., 2000. Operational model for the Lake Kinneret system. WaterShed Unit, Mekorot, Sapir Site, Israel. (in Hebrew).

Dalinsky, P., 1969. The salinization mechanism of Lake Kinneret- a research for the period 1912-1968. No. 746, Water Planning for Israel (Tahal), Tel-Aviv. (In Hebrew).

Eckhardt, K., 2005. How to Construct Recursive Digital Filters for Baseflow Separation. Hydrological Processes. 19, 507-515.

Gilad, D. and Schwartz, S., 1978. Hydrogeology of the Jordan sources aquifers. Isr. Hydrol. Serv. Rep. Hydro/5/78 58 pp. (in Hebrew).

Gilad, D. and J. Bonne 1990. Snowmelt of Mt. Hermon and its contribution to the sources of the Jordan River. Journal of Hydrology 114, (1/2), 1-15.

Goldshmidt, M.J., Arad A., Neev, D., 1967: The mechanism of the saline springs in the Lake Tiberias depression. Min. Dev. Geol. Surv., Jerusalem, Hydrol. Pap. #11, Bull. 45. 19 pp.

Gur, D., Bar-Matthews, M., Sass, E. 2003. Hydrochemistry of the main Jordan River sources: Dan, Banias, and Kezinim springs, north Hula Valley, Israel. Isr. J. Earth Sci. 52: 155–178.

Gvirtzman, H., Garven, G., Gvirtzman, G., 1997. Hydrogeological modeling of the saline hot springs at the Sea of Galilee, Israel. Water Resources Research, 33(5): 913-926.

Israel Hydrological Service, Annual Report, 2002. The development, usage, and situation of water resources in Israel until 2001, Israel Hydrological Service, ISSN-0793-1093, Jerusalem. 294pp. (in Hebrew).

Jeannin, P-Y. and Grasso, D.A., 1997. Permeability and hydrodynamic behavior of karstic environment. In "Karst Waters Environmental Impact", G. Gunay and A.I. Johnson [Eds.]. A.A. Balkema, Roterdam, Netherlands. pp. 335–342.

Mekorot,1987-2000. The annual water-solute-energy balances of Lake Kinneret. WaterShed Unit, Mekorot, Sapir Site,Israel. (in Hebrew).

Mero, F., 1978. Hydrology, In: C. Serruya [Ed.], Lake Kinneret, Monographiae Biologicae, Dr. W Junk, vol 32 pp. 88-102.

Mero, F. and S. Mandel. 1963. The hydrological mechanism of the saline springs of the western shore of Lake Kinneret. -*Tahal report 2399, Tahal,* Tel-Aviv, 10 pp (In Hebrew).

Mero, F., Simon, E., 1992. The simulation of chloride inflows into Lake Kinneret. J. Hydrol., 138: 345-360.

Michelson, H. 1975. Geohydrology of the enclave and the southeastern flanks of Mount Hermon. TAHAL 01/75/05 (in Hebrew).

Mualem Y. and G. Dagan, 1976. Methods of predicting the hydraulic conductivity of unsaturated soils. Research report to the BSF, Technion, Haifa, Israel.

Ponce, V.M., 1989. Engineering Hydrology- principles and Practices, Prentice Hall, Englewood Cliffs, New Jersey.

Rimmer, A., 1996. The salinity of Lake Kinneret: Estimation of the un-measured saline springs inflow characteristics. WaterShed Unit, Mekorot, Sapir Site, Israel. (in Hebrew).

Rimmer, A., Hurwitz, S., Gvirtzman, H., 1999. Spatial and temporal characteristics of saline springs: Sea of Galilee, Israel. Ground Water, 37(5): 663-673.

Rimmer, A. 2003. The Mechanism of Lake Kinneret Salinization as a Linear Reservoir. Journal of Hydrology, 281/3 pp. 177-190.

Rimmer, A. and G. Gal, 2003. The saline springs in the Solute and Water Balance of Lake Kinneret, Israel. Journal of Hydrology, 284/1-4 pp. 228-243.

Rimmer, A., M. Boger, Y. Aota and M. Kumagai, 2006. A Lake as a Natural Integrator of Linear Processes: Application to Lake Kinneret (Israel) and Lake Biwa (Japan). Journal of Hydrology, 319/1-4 pp. 163-175.

Rimmer, A., Y. Salingar. 2006. Modelling precipitation-streamflow processes in Karst basin: The case of the Jordan River sources, Israel, Journal of Hydrology (in press).

Simon, E., Mero, F., 1992. The salinization mechanism of Lake Kinneret. Journal of Hydrology, 138: 327-343.

Simpson, B., Carmi, I. 1983. The hydrology of the Jordan tributaries (Israel). Hydrographic and isotopic investigation. J. Hydrol. 62: 225–242.

Singh, V.P., 1988. Hydrologic systems, rainfall-runoff modeling. Prentice Hall, NJ.

Sugawara, M. 1995. Tank Model, in "Computer Models of Watershed Hydrology". Singh V.P. [Ed.]. Water Resources Publications, Colorado, pp. 165–214.

TAHAL (Water Planning for Israel). 1968-1986. The Annual Water-Solute-Energy Balances of Lake Kinneret. Tahal, Tel-Aviv. (in Hebrew).

Viney, N.R., and Sivapalan, M., 2000. LASCAM user manual, Centre for Water Research, University of Western Australia.

Wetzel, R.G., 1983. Limnology. Saunders College Publishing, Fort-Worth, 767 pp.

Winter, T. C., Uncertainties in Estimating the Water Balance of Lakes. *Water Resour. Bull.*, 17(1), 82-115, 1981.

Table 1: Summary of three system hydrological tools for the UCJR and LK.

Characteristic	1. Hermon hydrology	2. LK water-solute-heat balances	3. LK salinity
Time interval	day	month	year
input	Daily extrapolated rainfall and potential evaporation from stations south of Mt. Hermon.	Saline springs inflows, the salinity of the springs, and the evaporation.	Annual stream inflows, outflows, evaporation, direct annual rainfall. Average stream salinity;
output	Calculated base flow and surface flow components of 3 streams in the Hermon karst basins.	All the measured variables from the water, solute and heat balance, including measured inflows and outflows, and the measured monthly differences between storage of water, solute and heat in the lake.	Long-term predictions of solute mass, volume and salinity of the lake.
system	Hydrological model for karst environment, including 4 modules: the surface layer, surface flow, vadose zone, and groundwater.	A well known set of physical equations and assumptions which summaries the mass, solutes and energy balances of the lake.	The equations of complete mixing in which solute flux through the outlet is linearly proportional with solute storage.
Type of problem	An **inverse problem** of the type **identification**	An **inverse problem** of the type **detection**	A **direct problem** of **prediction**.
References	Rimmer and Salingar. 2006.	Assouline 1993.	Rimmer 2003.
Objective	**Identify** an appropriate system model for both the base flow and the surface flow components of a karst basin, and get better quantitative understanding of Mt. Hermon hydrology.	Calculate systematically the monthly water-solute-heat balances, and **detect** the three unknown inputs: evaporation, springs discharge and salinity.	To use an existing well-known physical mechanism of complete mixing as a tool to **predict** long-term changes of chloride concentration in the lake.
Applied to the period:	**1969-2005**	**1987-2005**	**1964-2005**

Figure captions

Figure 1: Schematic description of systems type problems.

Figure 2: a. Orientation map of the east Mediterranean. B. The direct watershed of Lake Kinneret (Dark) and the Upper Catchments of the Jordan River. C. Mt. Hermon area, and the Dan, Hermon and Senir watersheds.

Figure 3: Full Natural Flow (FNF) of the Dan, Hermon and Senir streams, and the application of the baseflow separation technique (BFS).

Figure 4: Schematic description of the Mt. Hermon conceptual hydrological model: Module 0 is the surface layer, Module 1 represents the vadoze zone, Module 2 consists of four groundwater reservoirs, and Module 3 simulates the surface flow. The calculated baseflow and the surface flow components of each tributary result in their full natural flow.

Figure 5: The predicted surface flow of the Hermon and Snir streams (C) compared to the surface flow from separation analysis (M) for the years 1991 to 1995.

Figure 6: The predicted baseflow of the Hermon tributaries (C) compared with the baseflow from separation analysis (M) for the years 1991 to 2000.

Figure 7: The predicted FNF of the three tributaries (C) compared to the measured flow (M) for the years 1991 to 2000.

Figure 8: The cumulative calculated full natural flow of the Jordan River compared to the measured cumulative full natural flow from 1969 to 2001.

Figure 9: Schematic diagram of water balance components, including inflows, outflows, and changes of lake volume. The unknown variables are marked with dashed box.

Figure 10: The residual of the Lake Kinneret water balance for the years 1986-2001: a. Monthly evaporation; b. monthly discharge from the un gauged saline springs.

Figure 11: Lake salinity (top panel) and solute mass in the lake (bottom panel) at the beginning of each year (1-st of October) for the years 1960-1999. (1) Operation of the Saline Water Carrier (SWC); (2) the winter of 1968-1969; (3) the winter of 1991-1992; (4) High lake salinity during

the years 1960-1963; (5) Expected lake salinity with the diversion of the saline springs by the SWC.

Figure 12: The complete mixing concept: C the salinity of the lake (ppm Cl^-), V volume (Mm^3), S the solute mass in the lake (kg), S_{in} and S_{out} the inflow (tributaries, springs) and outflow (pumping and water release) of solute, respectively ($kg \times year^{-1}$).

Figure 13: The changes of solute mass (left) and the changes of the salinity of the lake (right) a. from 1964 to 1987; b. from 1988 to 1999.

Figure 14: a. Predictions of lake salinity changes for five solute discharges (S_{in}=70, 90, 110, 130, 140×106 kg). Predictions were calculated with Qout=500 Mm^3 and initial salinity of $Clake_0$=280 ppmCl- for two lake volumes 1. V=3600 Mm^3 (solid line), and 2. V=4020 Mm^3 (dashed line). b. Predictions for 20 years of lake salinity changes as was calculated for four average outflows Q_{out}=200, 300, 400, and 500 Mm^3, with initial lake salinity C_{lake0}=230 ppmCl^-; V=4,020 Mm^3 ($S_0=924.6\times10^6$ kg) and $S_{in}=115\times10^6$ kg.

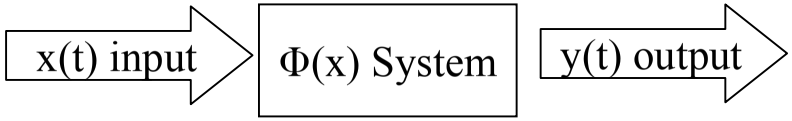

Type of Problem		Input	System	Output
Direct	Prediction	✓	✓	?
Inverse	Identification	✓	?	✓
Inverse	Detection	?	✓	✓

Figure 1

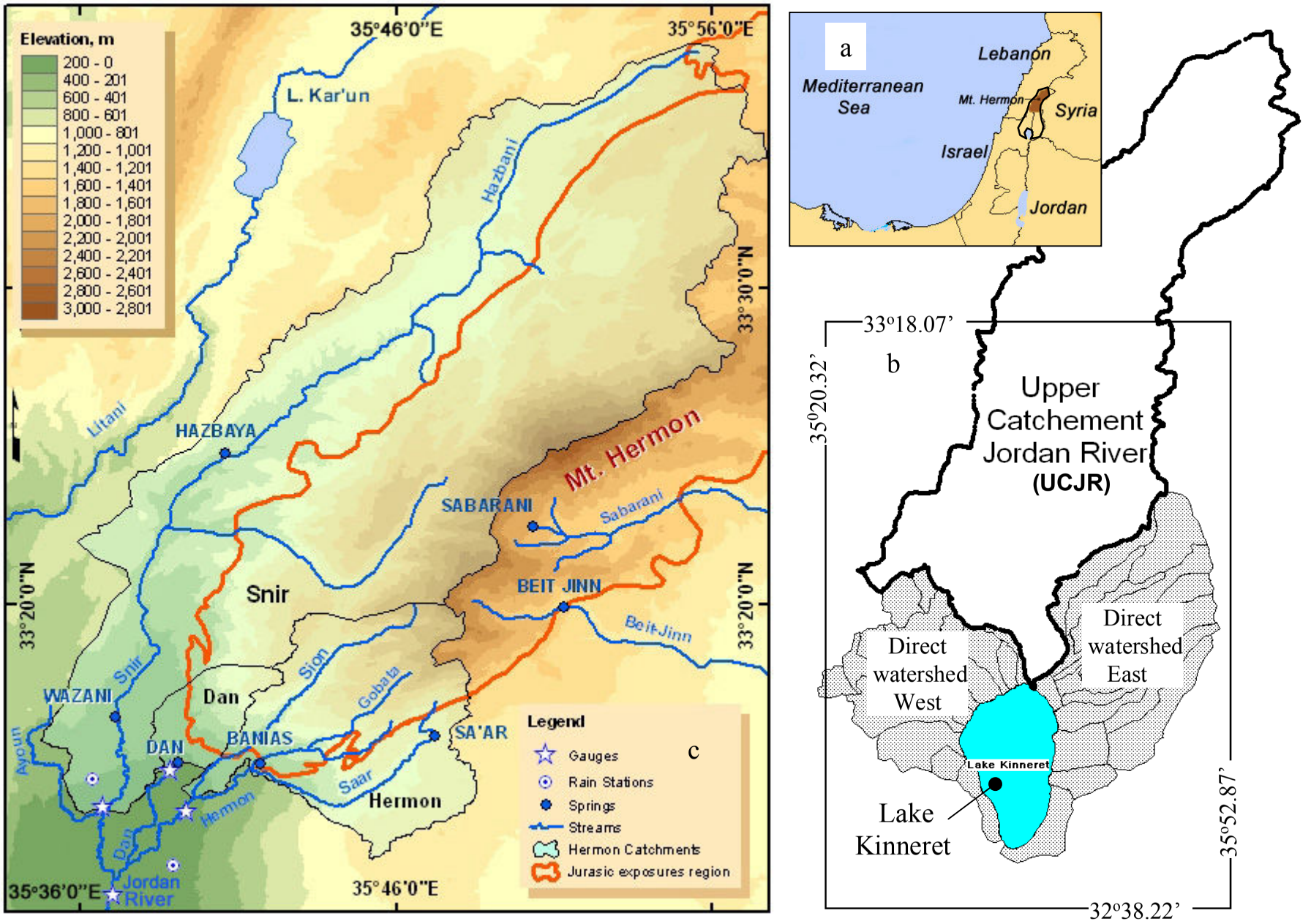

Figure 2

Rimmer

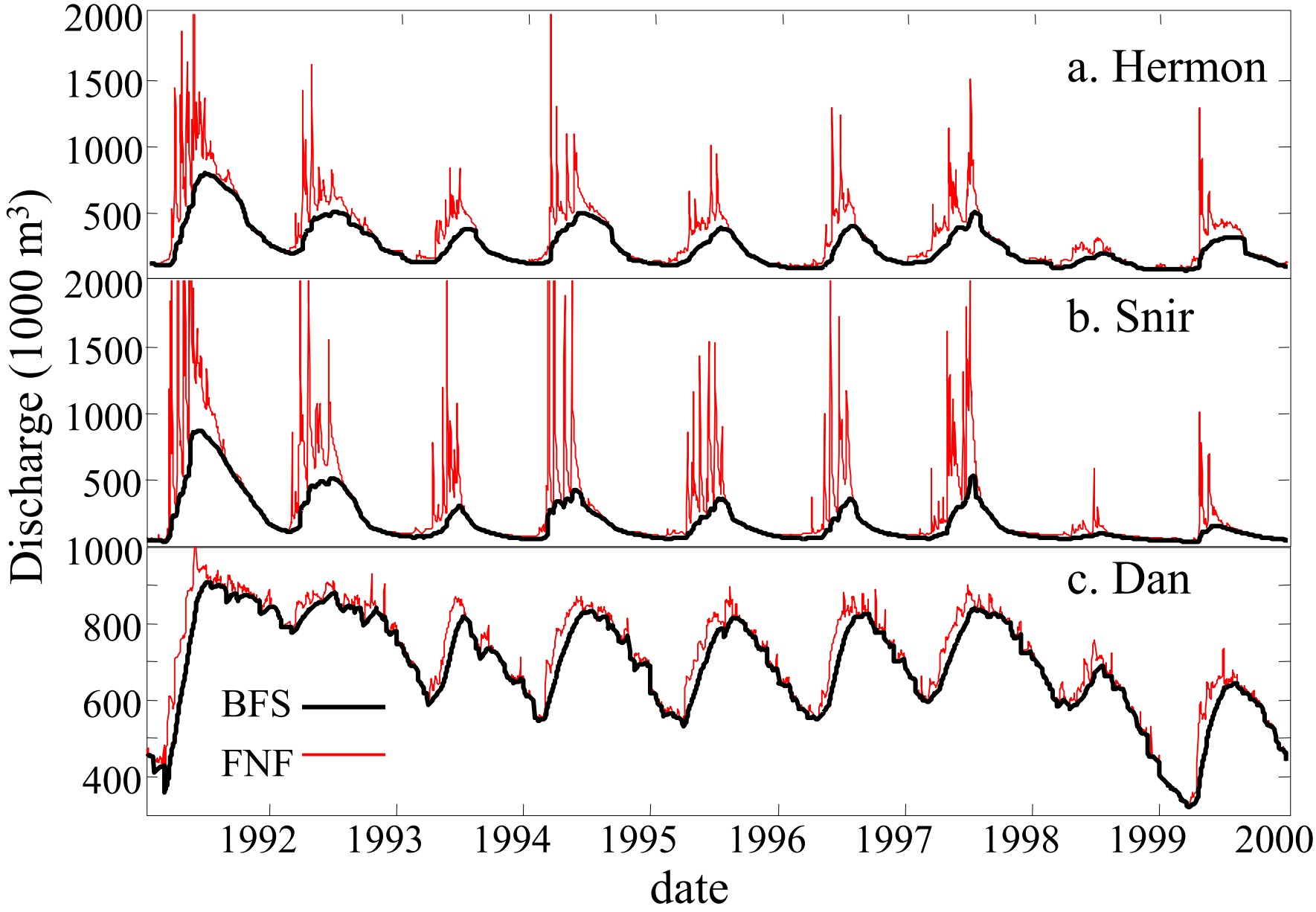

Figure 3

Rimmer

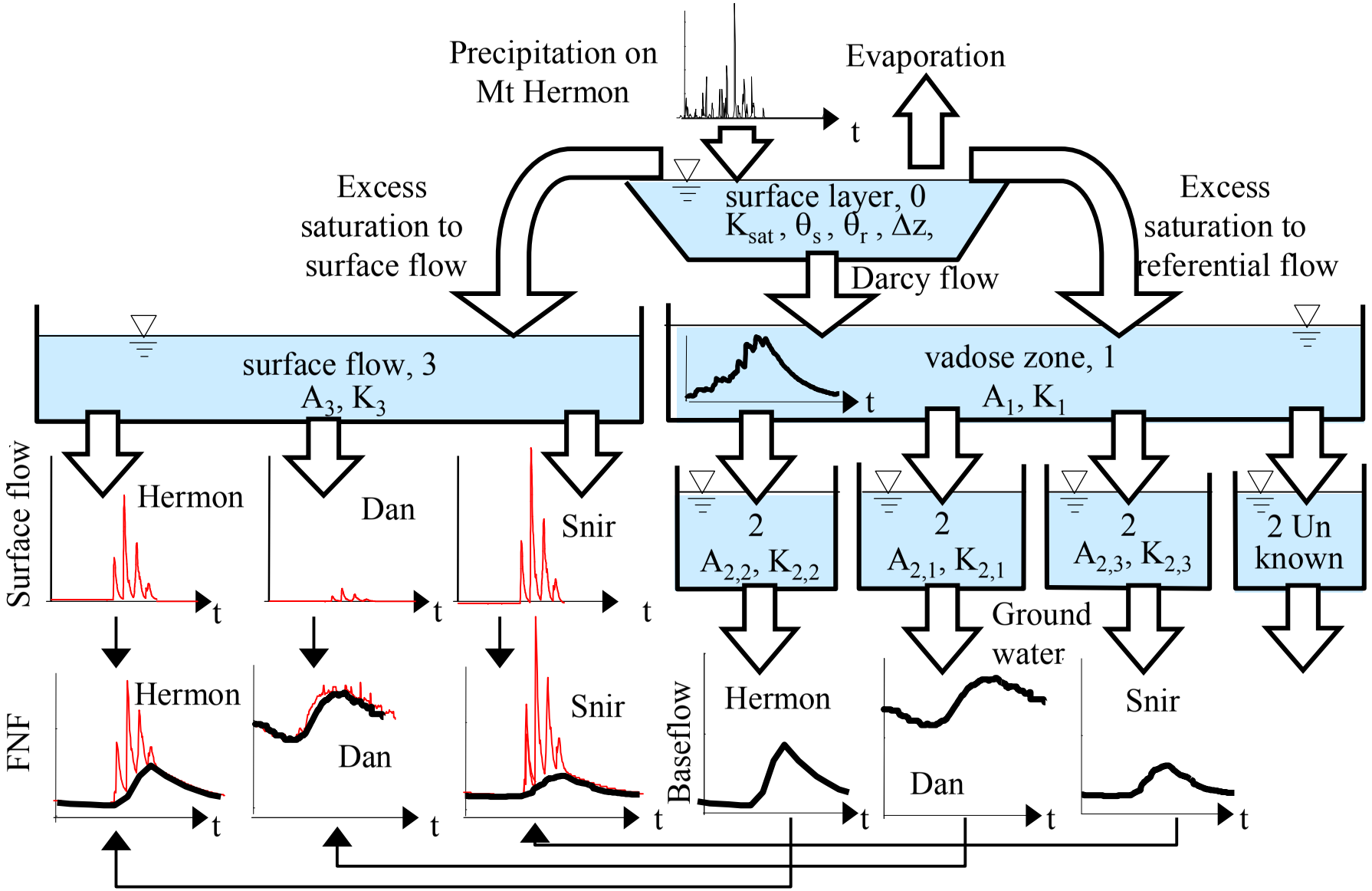

Figure 4

Rimmer

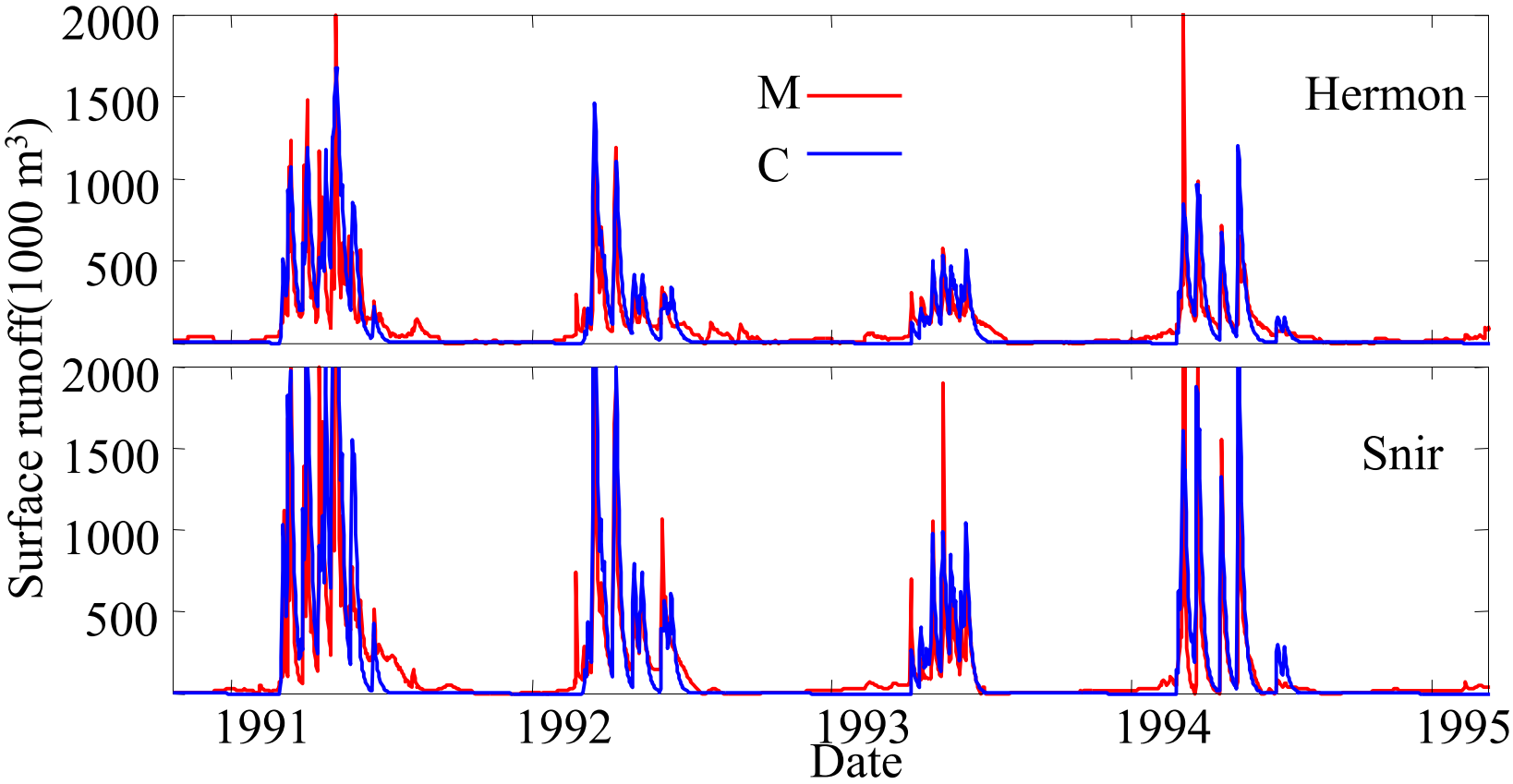
2000
1500
1000
500
Surface runoff(1000 m3)
M
C
Hermon
2000
1500
1000
500
Snir
1991
1992
1993
1994
1995
Date

Figure 5

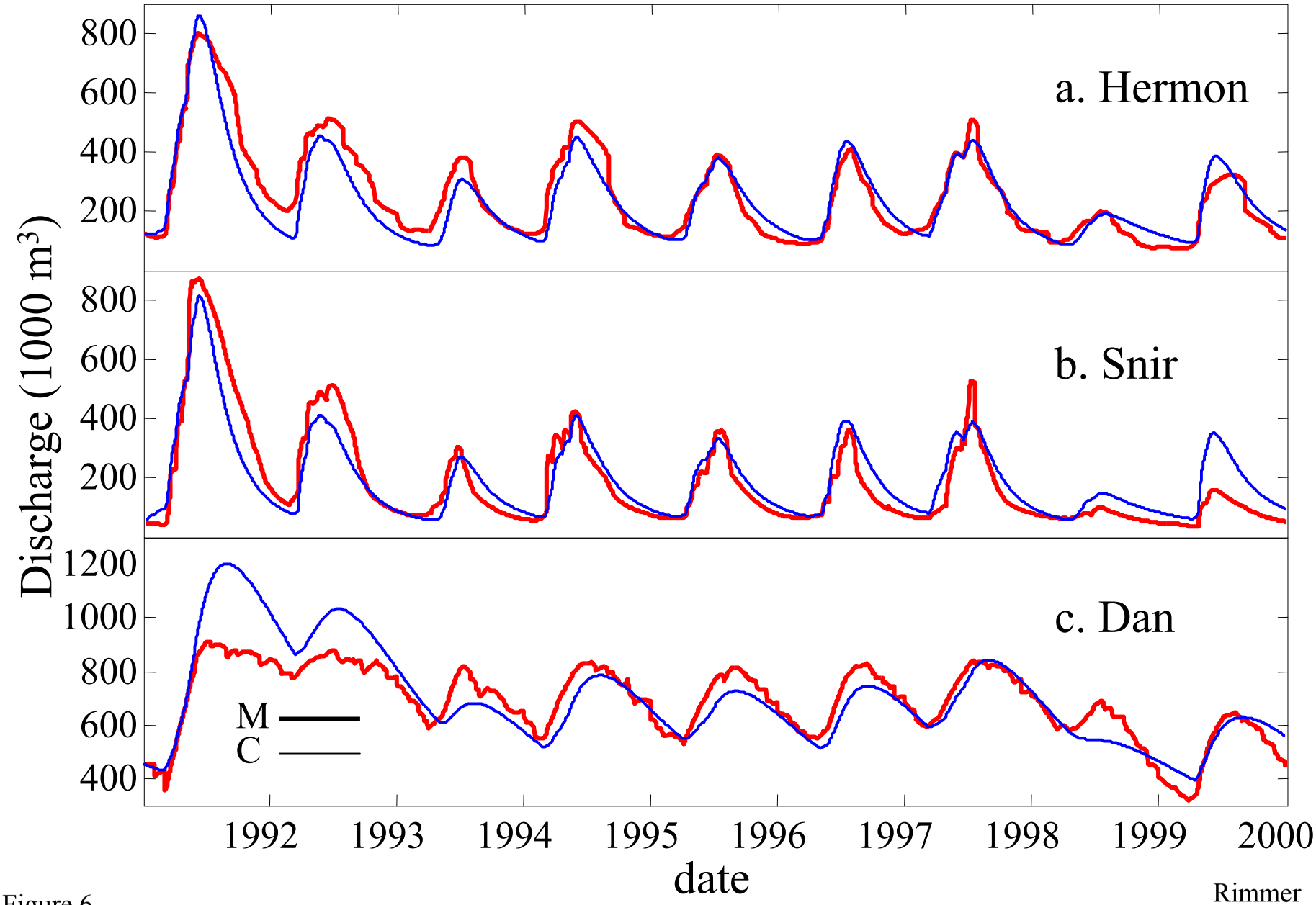

Figure 6

Rimmer

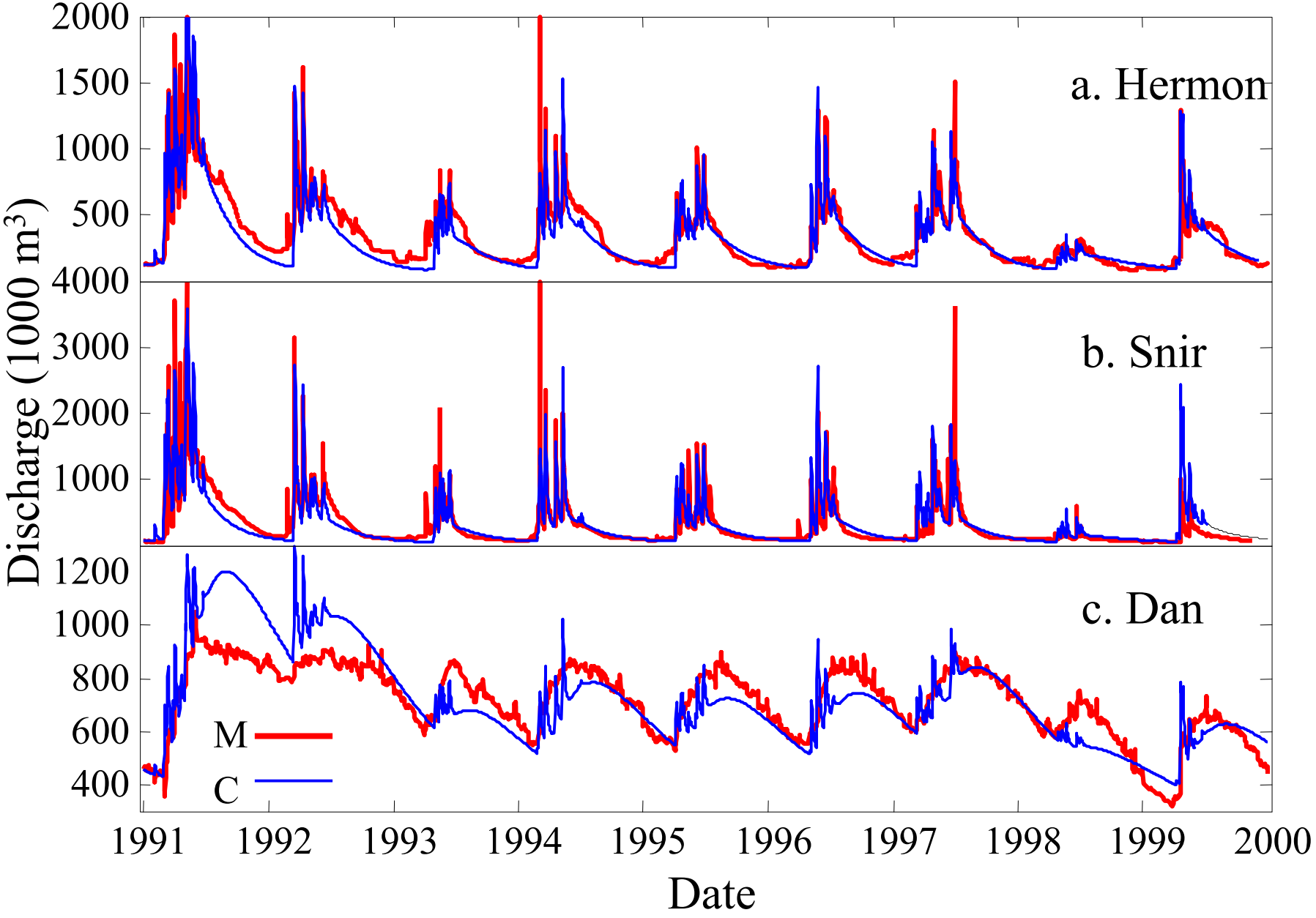

Figure 7

Rimmer

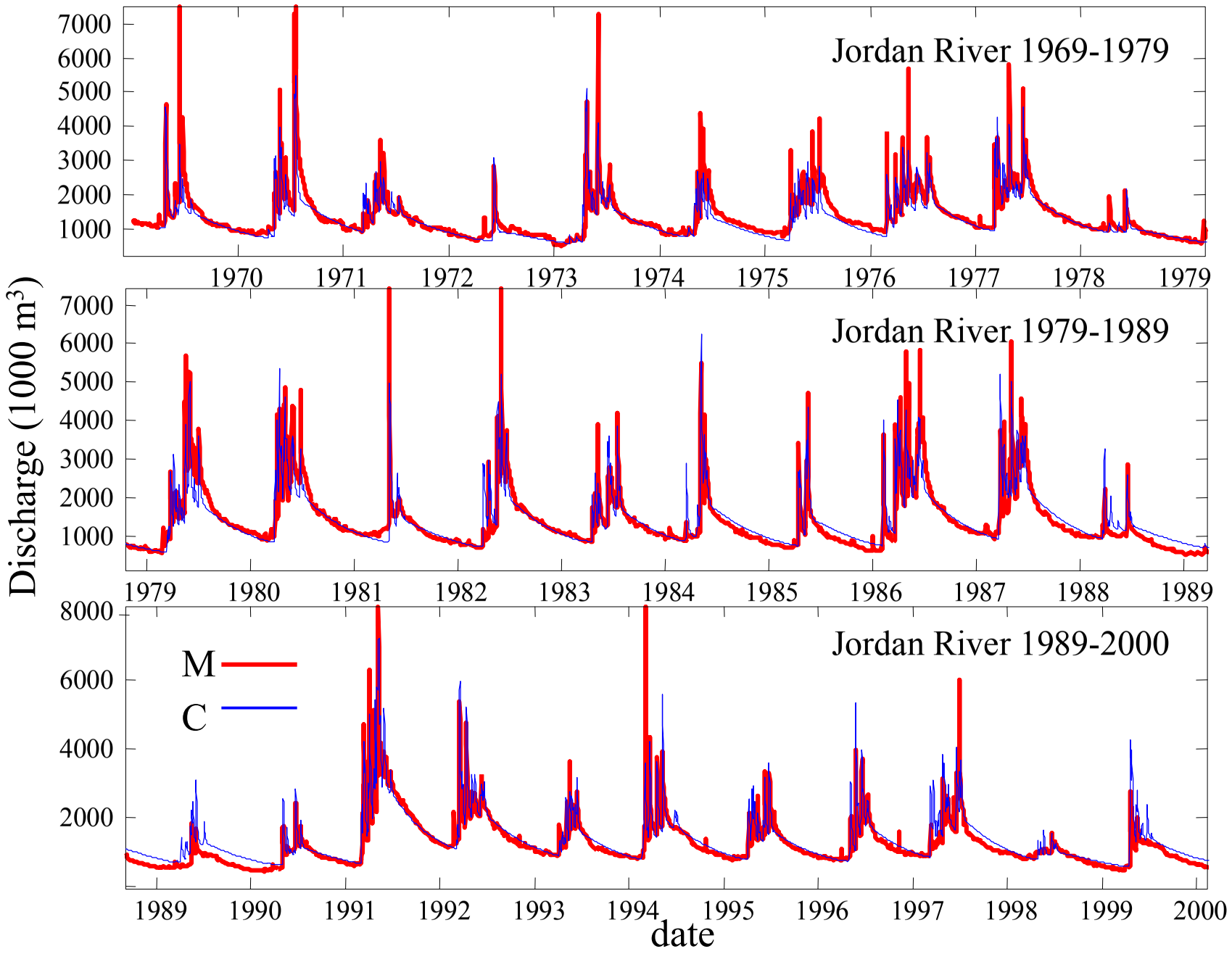

Figure 8

Rimmer

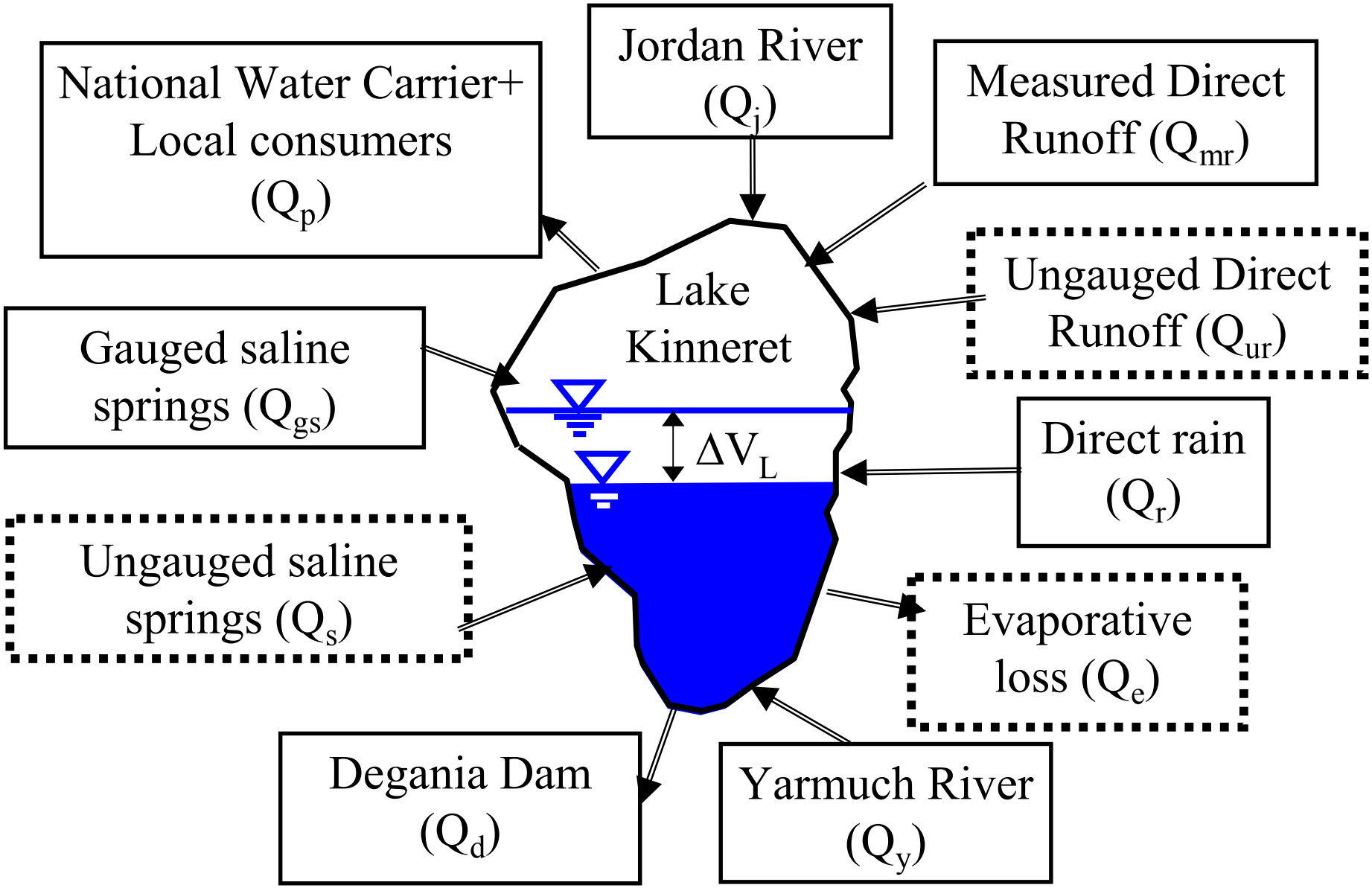

Figure 9

Rimmer

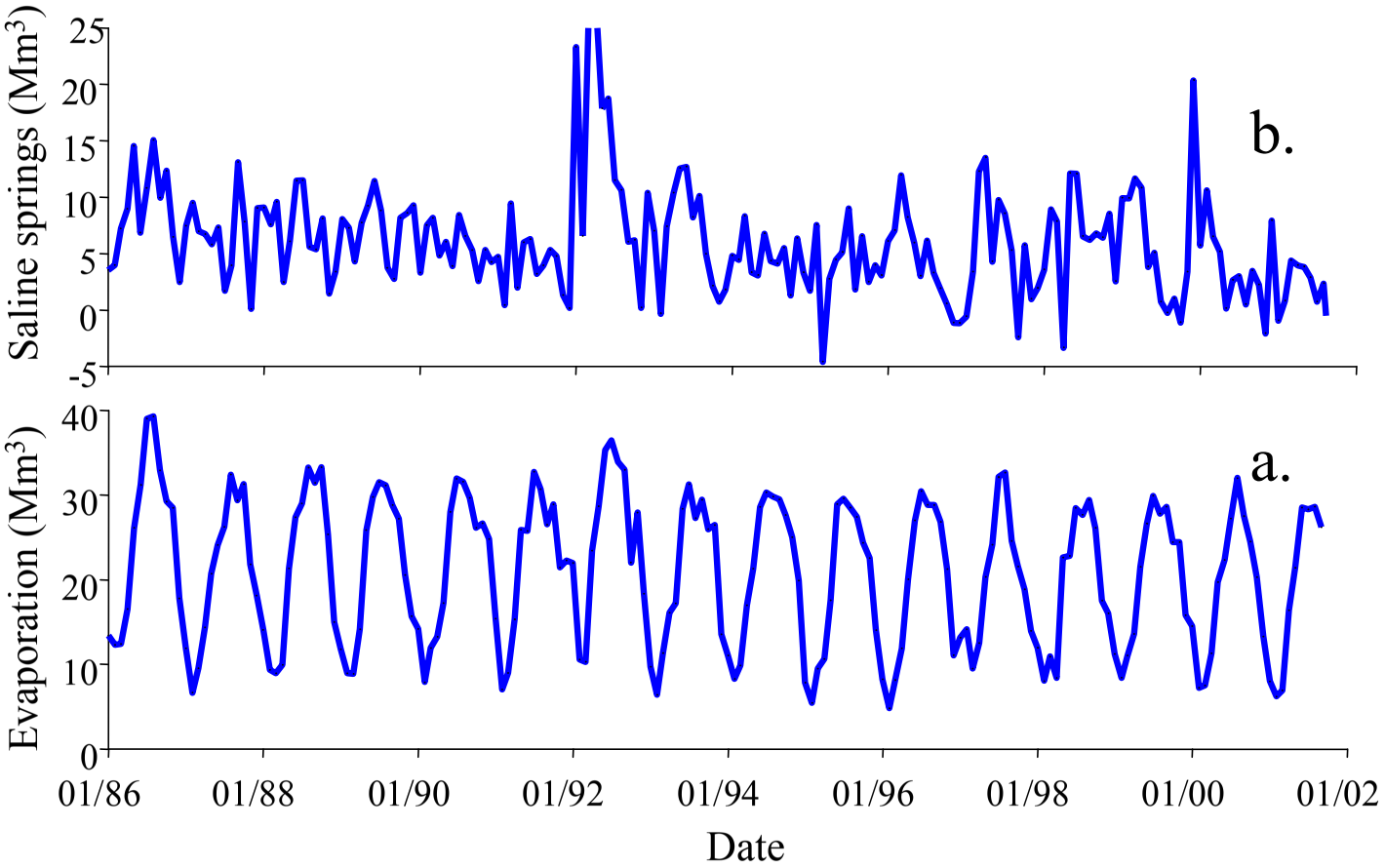

Figure 10

Rimmer

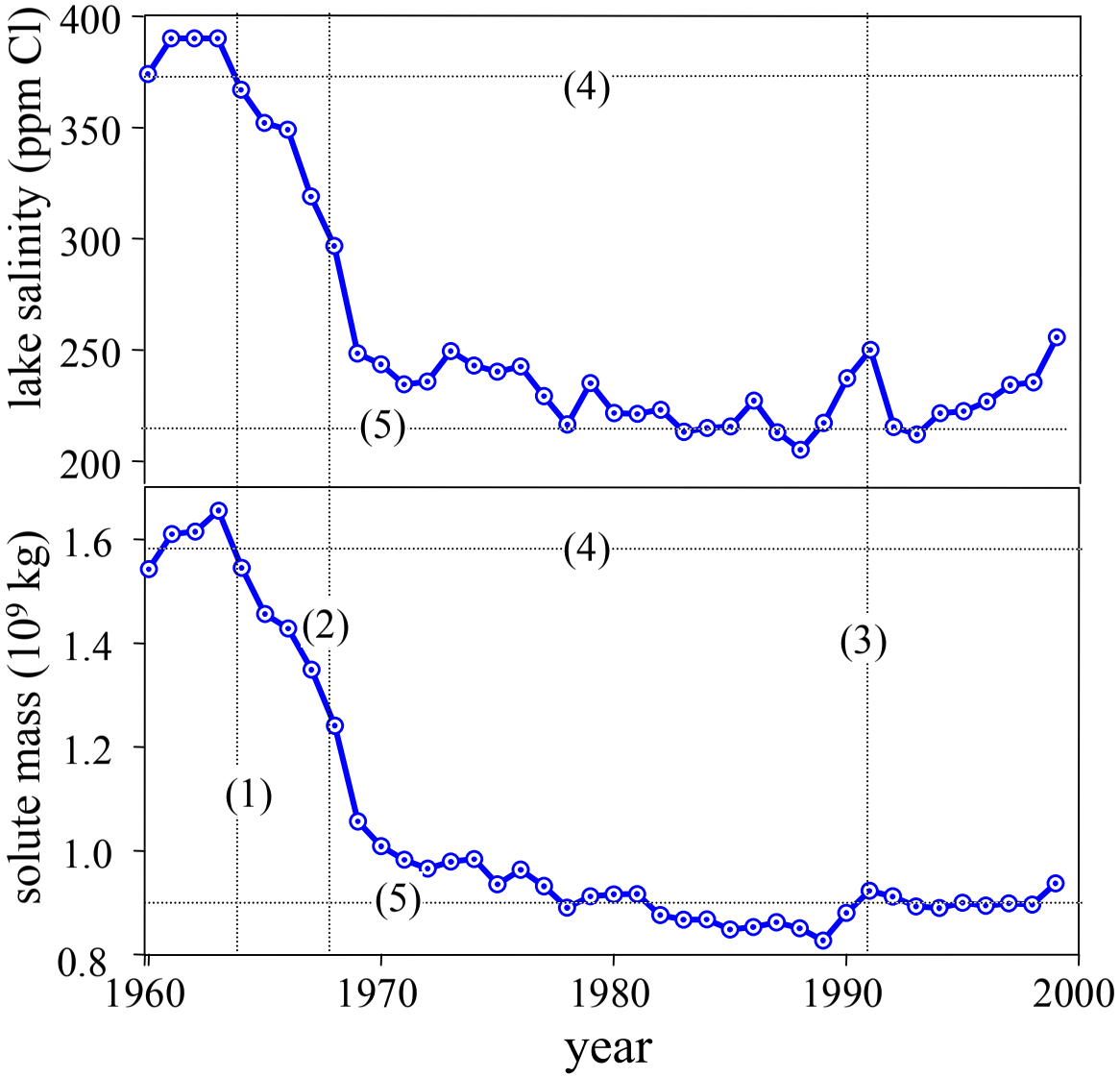

Figure 11

Rimmer

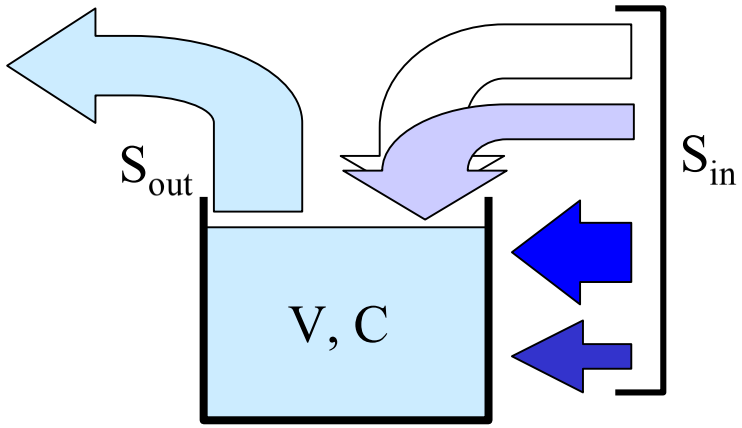

volume =V

Storage=S=V · C

Outflow=S_{out}=q ·S

Figure 12

Rimmer

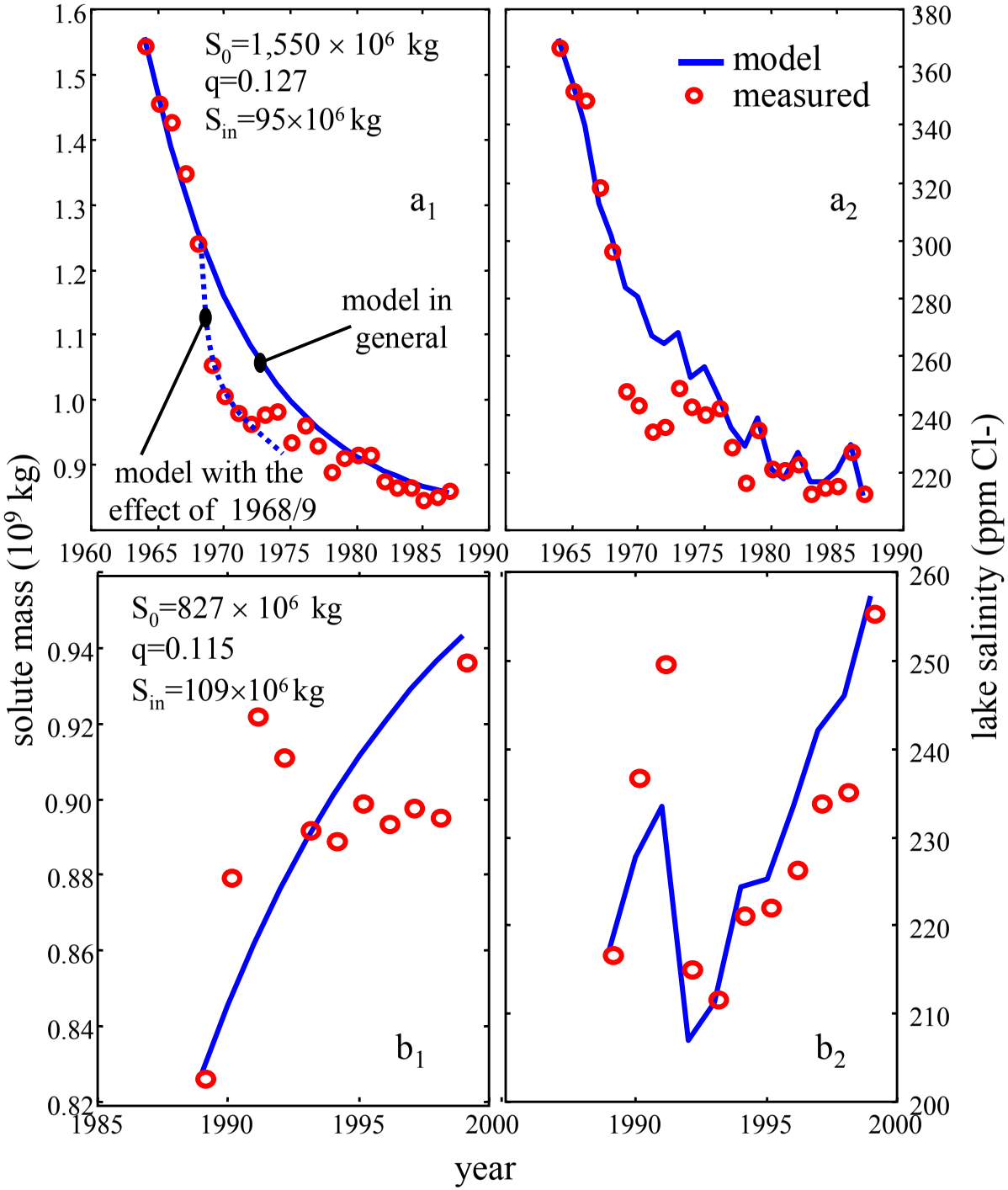

Figure 13

Rimmer

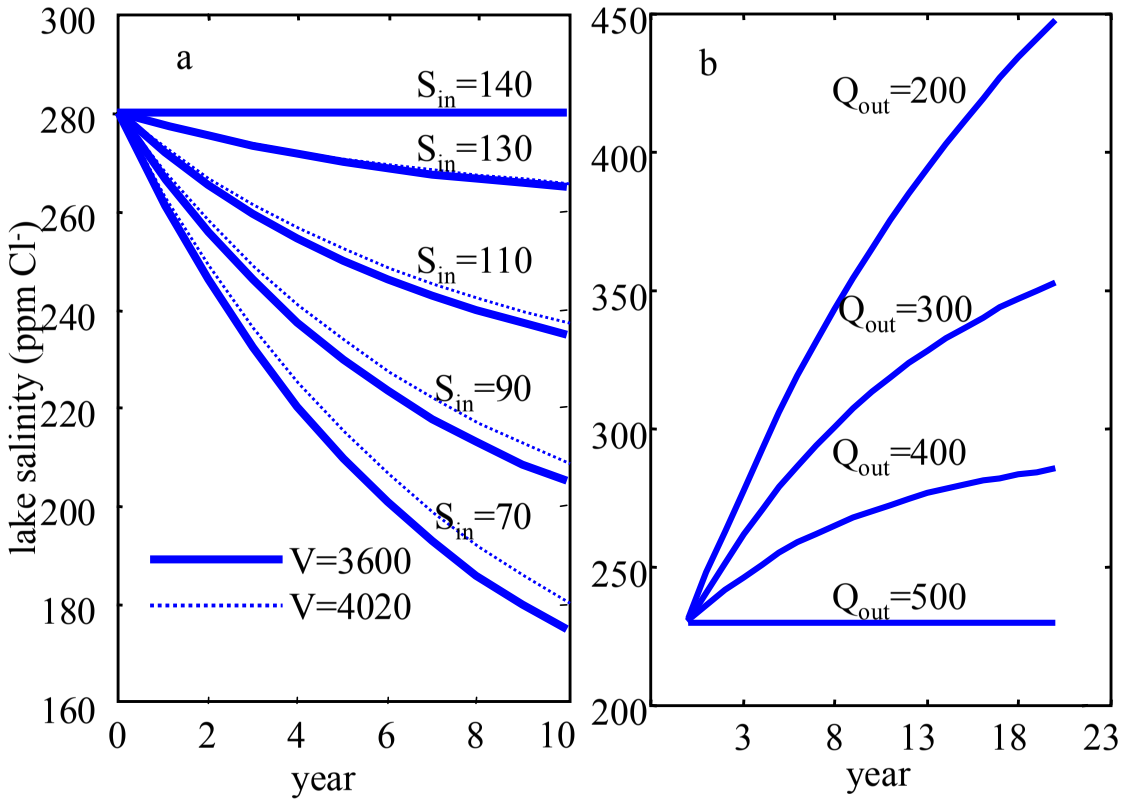

Figure 14

Rimmer